Flg22 regulates the release of an ethylene response factor substrate from MAP kinase 6 in *Arabidopsis thaliana* via ethylene signaling

Gerit Bethke[a], Tino Unthan[a], Joachim F. Uhrig[b], Yvonne Pöschl[a], Andrea A. Gust[c], Dierk Scheel[a,1], and Justin Lee[a,1]

[a]Leibniz Institute of Plant Biochemistry, Weinberg 3, D-06120, Halle, Germany; [b]Botanical Institute III, University of Cologne, Gyrhofstr. 15, D-50931 Cologne, Germany; and [c]Center for Plant Molecular Biology, University of Tübingen, Auf der Morgenstelle 5, D-72076 Tübingen, Germany

Edited by Klaus Hahlbrock, Max Planck Institute for Plant Breeding Research, Cologne, Germany, and approved March 30, 2009 (received for review October 10, 2008)

Mitogen-activated protein kinase (MAPK)–mediated responses are in part regulated by the repertoire of MAPK substrates, which is still poorly elucidated in plants. Here, the in vivo enzyme–substrate interaction of the *Arabidopsis thaliana* MAP kinase, MPK6, with an ethylene response factor (ERF104) is shown by fluorescence resonance energy transfer. The interaction was rapidly lost in response to flagellin-derived flg22 peptide. This complex disruption requires not only MPK6 activity, which also affects ERF104 stability via phosphorylation, but also ethylene signaling. The latter points to a novel role of ethylene in substrate release, presumably allowing the liberated ERF104 to access target genes. Microarray data show enrichment of GCC motifs in the promoters of ERF104–up-regulated genes, many of which are stress related. ERF104 is a vital regulator of basal immunity, as altered expression in both *erf104* and overexpressors led to more growth inhibition by flg22 and enhanced susceptibility to a non-adapted bacterial pathogen.

defense | elicitor | FRET | signal transduction

Mitogen-activated protein kinase (MAPK) cascades transduce external signals into cellular responses in eukaryotes (1). In plants, MAPKs orthologous to the *Arabidopsis* MPK3, MPK4, and MPK6 are activated by various stimuli including flg22, a bacterial flagellin–derived peptide that acts as a pathogen-associated molecular pattern (PAMP) (2–5). These three MAPKs control defense positively (MPK3/MPK6) (3, 6) or negatively (MPK4) (7).

Many phytohormones have been shown to affect defense responses; but most progress has been made in regard to salicylic acid (SA), jasmonic acid (JA) and ethylene (ET) (8). The tobacco MPK6 ortholog is activated by SA (9) and the *Arabidopsis mpk4* mutant has elevated SA levels and enhanced pathogen resistance (7). Genetic evidence linking ET to MAPK signaling is also suggested by the negative regulator of the ET response, Constitutive Triple Response 1 (CTR1), a Raf-like kinase that was recently shown to control MPK3/6 activation via MKK9 (MAPK kinase 9) (10). Both JA and the ET precursor, 1-aminocyclopropane-1-carboxylic acid (ACC), activate MPK6 in *Arabidopsis* (11, 12) but not in tobacco (13). Although responses may differ between plant species, the activation of MPK6 by ET/ACC is highly debated (14). In another report, ACC did not activate MPK6, but ET biosynthesis was positively regulated by MPK6 through posttranslational stabilization of the rate-limiting ACC synthase (ACS) isoforms, ACS2 and ACS6 (14, 15).

In addition to the cytoplasmic ACSs, MAPKs also target nuclear proteins (10, 16, 17); this may occur either after MAPK nuclear translocation following activation (18, 19) or as preformed nuclear protein complexes (20). The latter would imply movement of the upstream MKKs into the nucleus to modify the MAPKs or, alternatively, that the activated MAPKs enter the nucleus to displace the inactive MAPK from preformed complexes. Examples of nuclear targets include the MPK4 substrates, MKS1 and two MKS1-interactors of the WRKY transcription factor family, WRKY25 and WRKY33 (17). A MPK4/MKS1/WRKY33 complex is thought to control camalexin biosynthesis via the action of WRKY33 (20). MKS1 acts downstream of MPK4 to regulate the SA-dependent pathway but is not involved in the ET/JA pathway. However, as *mpk4* mutants are affected in JA/ET-mediated defense gene expression, additional unknown MPK4 substrates must be involved. Thus, the understanding of defense regulation via MAPKs is limited by the current knowledge of plant MAPK substrates. Using a yeast-2-hybrid screen, we identified a transcription factor of the Ethylene Response Factor family, ERF104, which interacted with MPK6. We validated this interaction *in vivo* and showed ERF104 to be a nuclear substrate involved in plant defense. The release of ERF104 from MPK6 in the nucleus required rapid ET signaling, which could indicate novel roles of hormone signaling in mediating substrate release.

Results

MPK6 and ERF104 Show Dynamic Interaction in Fluorescence Resonance Energy Transfer (FRET) Assays. The Ethylene Response Factor, ERF104 (At5g61600), interacted with MPK6 in a yeast-2-hybrid (Y2H) screen. A further hint of *bona fide* interaction is that MPK6-YFP, normally of nucleocytoplasmic distribution, became nuclear-localized when cotransfected with the nuclear-localized ERF104-CFP (Fig. 1*A*). These nuclear signals are not caused by cleavage products of fluorescent proteins, as Western blot showed intact fusion proteins [supporting information (SI) Fig. S1*A*]. The tagged proteins can also be activated by flg22 and hence are functional (Fig. S1*B*). Acceptor photobleaching-based FRET (21), initially tested with various positive and negative controls (Fig. 1, Fig. S1*C*), was used to validate the interaction. Positive FRET indicating *in vivo* protein–protein interaction occurred between ERF104 and MPK6 but not with MPK3 or MPK4 (Fig. 1*B*).

Loss of the FRET signal upon flg22 elicitation suggests MPK6/ERF104 complex disruption within 5–15 minutes (Fig. 1*B*), which could be validated to some extent by co-immunoprecipitation (Fig. S1*D*). By contrast, flg22 did not abrogate interaction between MPK6 and its upstream kinase MKK4, indicating that the flg22 effect is no FRET artifact, although not ruling out the existence of MKK4/MPK6 complexes in non-flg22-regulated pathways. No flg22-mediated disruption was seen by co-treatment with an excess of flg22 antagonist, flg15d5 (22) (Fig. 1*C*) or in *fls2*-derived protoplasts (Fig. S1*E*). Hence, flg22 perception via the FLS2

Author contributions: G.B., D.S., and J.L. designed research; G.B., T.U., and J.F.U. performed research; A.A.G. contributed new reagents/analytic tools; G.B., T.U., Y.P., D.S., and J.L. analyzed data; and G.B., D.S., and J.L. wrote the paper.

The authors declare no conflict of interest.

This article is a PNAS Direct Submission.

Data deposition: The microarray CEL files in this paper have been deposited in the Gene Expression Omnibus (GEO) database, www.ncbi.nlm.nih.gov/geo (accession no. GSE11807).

[1]To whom correspondence should be addressed. E-mail: jlee@ipb-halle.de or dscheel@ipb-halle.de.

This article contains supporting information online at www.pnas.org/cgi/content/full/0810206106/DCSupplemental.

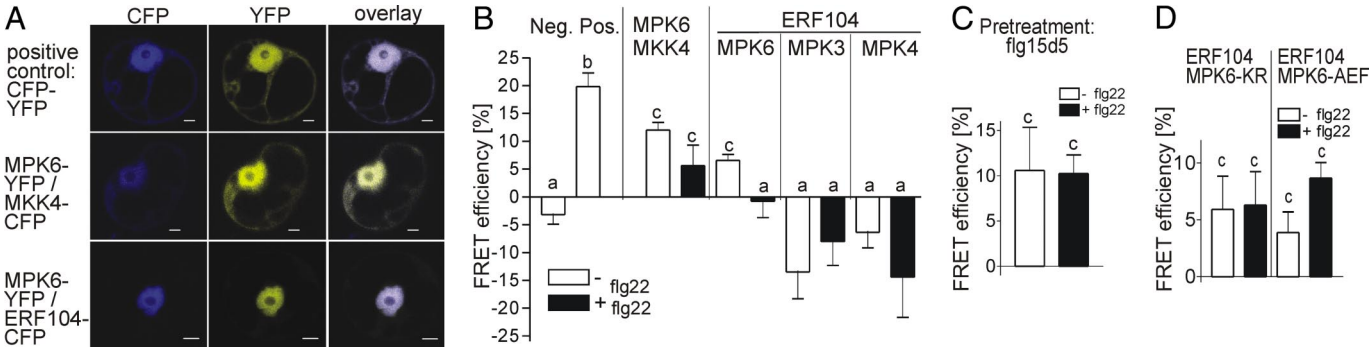

Fig. 1. *In vivo* protein-protein interaction based on FRET analysis. (*A*) Localization of the indicated tagged proteins in transfected *Arabidopsis* protoplasts. Scale bar, 5 μm. (*B*) FRET analysis of the indicated components. A CFP-YFP fusion (positive control) and CFP alone (negative control) served as the reference. Note that data with no interaction typically show negative values because of donor bleaching during imaging. The statistical significance is indicated (Mann-Whitney test: samples with the same letters are not significantly different). (*C*) Co-treatment with inactive flg15d5 peptide (300 μM) blocks the ability of flg22 to disrupt the MPK6/ERF104 complex. (*D*) Kinase-inactive MPK6s interacted with ERF104 independently of flg22 treatment (mutations in ATP-binding pocket, MPK6KR [$K_{92}R$], or activation loop, MPK6AEF [$S_{229}A$, $S_{232}A$]). In (*B-D*), analysis was performed before (white bars) or after flg22 treatment (5–15 minutes; black bars).

receptor is needed. In addition, MPK6 activity is required for the flg22-mediated disruption, as inactive MPK6 variants (mutations in ATP binding pocket, MPK6KR, or the activation loop, MPK6AEF) interacted with ERF104 despite flg22 treatment (Fig. 1*D*).

ET Signaling Affects ERF104/MPK6 Interaction. The ET precursor, ACC, had no effect on the positive control (Fig. S1*F*) but reduced the ERF104/MPK6 FRET signal (Fig. 2*A*). The ACC effect is lost in ET-insensitive mutants (Fig. 2*B*) and hence is caused by ET signaling. To determine the role of ET signaling, protoplasts were pretreated with aminoethoxyvinylglycine (AVG, an ACS inhibitor) or silver ions (ET perception inhibitor) for 10 minutes before flg22 stimulation. Both treatments blocked the flg22-induced loss of FRET (Fig. 2*A*). Flg22 disruption of the ERF104/MPK6 complex was abrogated in strong ET-insensitive mutants (*ein2* or *ein3/eil1*) (Fig. 2*B*) but not in weaker mutants (*ein3* or *etr1*, Fig. S2*A*). Hence, the disruption of MPK6/ERF104 interaction by flg22 requires ET biosynthesis and signaling.

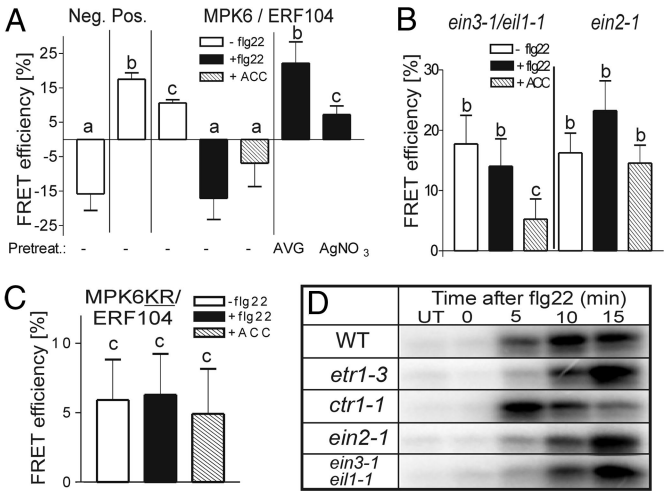

Fig. 2. Role of ET and MPK6 activity in the ERF104/MPK6 interaction. (*A*) To study the role of ET signaling in ET-insensitive mutants required the use of plant-derived protoplast. FRET was first tested in protoplasts of wild-type *Arabidopsis* to show that leaf- and cell-culture-derived protoplasts show similar results in FRET (*cf.* Fig. 1*B*). Besides flg22 (black bars), ACC treatment (shaded bars) also disrupts the MPK6/ERF104 complex. Pretreatment with AVG or $AgNO_3$ abrogated the flg22-mediated disruption. Letters above each bar mark the statistically distinct groupings as described in Fig. 1. (*B*) Genetic evidence, based on strong ET-insensitive mutants (*ein2–1* or the *ein3–1/eil1–1* double mutant), showed that ET signaling is required for loss of FRET after flg22 or ACC addition. (*C*) Lack of ERF104/MPK6KR complex disruption by flg22 treatment is not caused by dominant-negative interference of the inactive MPK6 on ET biosynthesis, as ACC addition would otherwise replace this function. (*D*) MPK6 activity in various genetic background was measured by immune-complex MBP kinase assays. Minor changes in the activity kinetics are experimental variations and unlikely to be real differences (A representative of 3 experiments is shown). UT = untreated.

Is ET Upstream or Downstream of MAPK Activation? There are conflicting viewpoints in regard to this issue (10, 12, 14, 24, 25), wherein ACC activation of MAPKs including MPK6 (10, 12) is disputed (14). We re-evaluated the ability of ACC to activate MAPK but no rapid MPK6 activation, based on the sensitive immune-complex kinase assay, was detected (not shown). Enhanced MPK6 activity in the *ctr1* mutant (10, 12) was also not seen (Fig. 2*D*), which may be caused by different experimental procedures such as the use of transfected *ctr1* protoplasts (10) compared with intact unstressed seedlings in our system. Reduction of ET production by preincubation with AVG before flg22 stimulation had no or only marginal effects on MPK6 activation (Fig. S2*B*). Although minor delay/reduction of MPK6 activation by flg22 is seen in the various ET signaling mutants (Fig. 2*D*), this varied between experiments and, more importantly, it is not completely blocked. Thus, our data do not support ET being upstream of MAPK6 activation, but in agreement with Liu and Zhang (14), imply that the rapid flg22-induced ET signal lies downstream of MPK6 activation.

ERF104 Is an MPK6 Substrate. ERF104 possesses two potential MAPK phosphorylation sites (26) (Fig. 3*D*). When ERF104-HA was co-expressed with a constitutive active (CA) MKK5 (19) (which

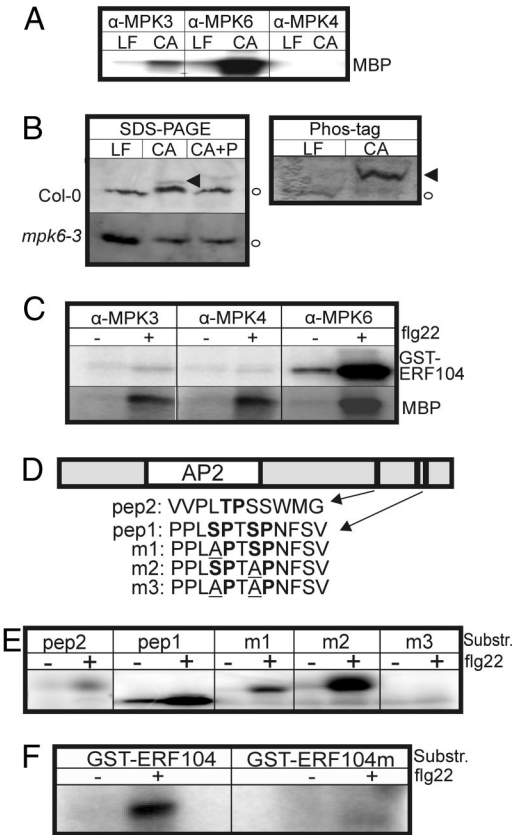

Fig. 3. MPK6 phosphorylates ERF104. (*A*) MBP kinase assays with immunoprecipitated MAPKs showing that transfection with a ''constitutive-active, CA,'' but not an inactive ''loss-of-function, LF,'' MKK5 led to the activation of MPK3/MPK6 but not MPK4. (*B*) Western blot showing that *in vivo* MPK3/MPK6 activation by CA-MKK5 (but not the LF form) led to a second band of HA-tagged ERF104 (triangle). This band is lost when a phosphatase (At2g40180) is included (CA+P) and is not seen in *mpk6*-derived protoplasts (*bottom*). The *right panel* shows enhanced mobility shift of the upper band in gels with polymerized Phos-tag, which retards mobility of phosphorylated proteins in SDS-PAGE. (*C*) Recombinant GST-ERF104 protein is phosphorylated *in vitro* by active MPK6, but not MPK3 and MPK4, immunoprecipitated from flg22-elicited *Arabidopsis*. The activities of the three kinases are shown by using the general substrate, MBP (*lower panel*). No MPK6 activity was precipitated from *mpk6* plants (Fig. S2*C*), showing the specificity of the assay. (*D*) Scheme of the AP2-domain in ERF104 and sequence of peptides used for kinase assays. Pep1 (amino acid 226–237) and pep2 (amino acid 202–212) contain two or one predicted MAPK phosphorylation sites, respectively. (*E*) The peptides (in *D*) were used as substrates for *in vitro* assays with immunoprecipitated MPK6. Pep1 served as substrate, whereas pep2 is only weakly phosphorylated. Pep1 derivatives, m1 and m2, are still phosphorylated but with different strength, while m3 is no longer used as substrate (*lower panel*). (*F*) Full-length GST-ERF104m (mutated to correspond to pep1m3) is no longer phosphorylated by MPK6.

activated MPK3 and MPK6 but not MPK4, Fig. 3*A*), an additional ERF104-HA band of reduced mobility appeared. This was not seen with the corresponding inactive MKK5-LF or when performed in *mpk6* background (Fig. 3*B*). The inclusion of a protein phosphatase (At2g40180), as a third transfection component, eliminated this upper band. In "Phos-tag" gels, a method for retarding mobility of phosphoproteins in sodium dodecyl sulfate–polyacrylamide gel electrophoresis (SDS-PAGE) (27), the mobility shift was enhanced (Fig. 3*B*). Moreover, MPK6, but not MPK3 or MPK4, immunoprecipitated from flg22-treated cells, accepted recombinant GST-ERF104 as substrate (Fig. 3*C*). Hence, ERF104 is specifically phosphorylated by MPK6.

Two synthetic peptides spanning the putative phosphorylation sites (26) were tested as substrates (Fig. 3*D*). Pep2 was marginally, whereas pep1 was strongly, phosphorylated (Fig. 3E). When both serines within the (S/T)P motifs in pep1 were exchanged by alanine, no phosphorylation was seen; if only one was mutated, the first motif appeared to be the major phospho-site (Fig. 3 *D* and *E*). When the two corresponding phosphorylation sites (encompassed by pep1) were altered in the full-length ERF104, the mutated ERF104 (ERF104m) was no longer phosphorylated by MPK6 (Fig. 3*F*). Although this suggests that one or both of these two sites is/are the major phospho-sites, the issue is complicated by the fact that no FRET was seen with ERF104m and MPK6 (Fig. S2*D*). However, MPK6-YFP is still remobilized to the nucleus when cotransfected with ERF104m (Fig. S2*E*), suggesting that interaction may still occur but is not detectable, perhaps because conditions required for FRET (e.g., transition dipole orientation for optimal energy transfer) are not met.

Mutated ERF104 Is a Functional Transcription Factor but Less Stable. Treatment of plants with cycloheximide to block protein synthesis revealed reduced stability of ERF104m compared with ERF104, especially after flg22 treatment (Fig. 4*A*). To appraise the effect of the mutations on the protein function, we first determined the ERF104 activity. It binds GCC-containing DNA probes in electrophoretic mobility shift assays (EMSA) with high specificity, as is shown by competition with an excess of unlabeled DNA, the failure of an unrelated WRKY binding element to compete this binding and the lack of binding to a mutated GCC element (Fig. S3*A*), or to S, DRE, G, JERE, and WRKY elements often found in promoters of various pathogen- and stress-responsive genes (28) (data not shown). In particular, the single nucleotide difference between S and GCC elements (Fig. 4*B*) highlights this specificity.

ERF104 was transiently expressed in protoplasts, which raised the activity of co-transfected synthetic promoter with GCC elements but not those with mutated GCC or the closely related S-Box element (Fig. 4*B*). Similarly, stably transformed *35S::ERF104* ($ERF104^{OE}$) plants show *GUS* expression in reporter lines with promoters containing GCC, but not other elements (28) (Fig. 4*C*). A weak GUS staining in plants with the JERE-promoter element is likely an indirect effect as ERF104 did not bind JERE elements. Thus, ERF104 activates promoters with GCC *cis*-acting elements.

In contrast to native ERF104, promoter activity is highly variable after transient expression of the mutated *ERF104m* and also slightly more variable in stable transgenic *35S::ERF104m* ($ERF104m^{OE}$) plants (Fig. S3*B* and *C*). This higher variation seen in protoplasts may be accounted by stress-induced instability of ERF104m (Fig. 4*A*). In summary, the transcription factor function in ERF104m is intact, but its stability is reduced upon stress (flg22) treatment. In line with this, the necrotic-like specks in older leaves, which are stainable by trypan blue (dead cells) and DAB (H_2O_2), in the $ERF104^{OE}$ lines were also seen in $ERF104m^{OE}$ lines but less frequently (Fig. S3*D*) and several tested ERF104-up-regulated genes were similarly expressed in the ERF104m lines (not shown).

Expression Profiling to Find Putative ERF104 Targets. To dissect the role of the MPK6/ERF104 protein complex in flg22 signaling, we profiled gene expression in *mpk6* and *erf104* mutants by microarray analysis. Most flg22-responsive genes were similarly regulated (Fig. S4*D*) and there was no clear trend of specific pathways being affected, suggesting that redundancies likely mask most of the effects in single mutants. In contrast, $ERF104^{OE}$ plants showed 534 up- and 17 down-regulated genes (at least 3-fold changes; False Discovery Rate, FDR, $P < 0.05$) (Table S1), with the strongest induction (≈1000 fold) for two *PDF1.2* genes (Table 1, Fig. S4*C*). The 1-kb upstream regions of genes up-regulated >10-fold by ERF104 are enriched for GCC elements (based on "Motiffinder"), suggesting these to be direct targets of ERF104. Indeed, chromatin immunoprecipitation (ChIP) showed occupation of the *PDF1.2* promoter by ERF104 (Fig. 5*A*). When compared with other

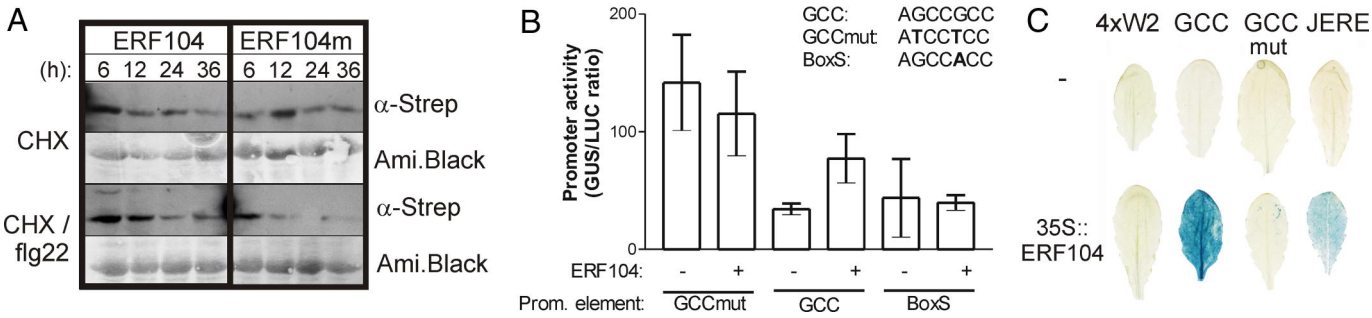

Fig. 4. ERF104 is a transcriptional activator, and ''phospho-site'' mutation reduces its stability. (*A*) ERF104m is less stable than ERF104. Transgenic plants of Strep-tagged ERF104 variants were treated with cycloheximide (to block protein synthesis) and the protein stability monitored by Western blot. Reduced stability of ERF104m is obvious mainly after flg22 treatment. (*B*) Plasmids with *GUS* driven by the indicated promoter elements were transiently transfected into protoplasts together with (+) or without (-) *35S::ERF104*. The promoter activity is shown as a ratio of the GUS activity normalized to that of constitutively expressed luciferase (LUC). The core binding sequences of the promoter elements are indicated. (*C*) Stable *35S::ERF104* transgenics were crossed into GUS reporter plants. GUS activity (blue staining) can be seen in crosses with the lines with GCC promoter elements but not with mutated GCC (GCCmut) or WRKY elements (4xW2). A weaker staining of plants with jasmonate-responsive elements (JERE) is likely an indirect effect as ERF104 does not bind to JERE elements in EMSA.

microarray data for signals that also target GCC elements, only a partial overlap with ERF1–up-regulated (29) or JA- or ET-responsive genes was found (Fig. S4*A*, Table S6), implying that pathways controlled by ERF104, ERF1, ET, or JA are not identical.

Many of the ERF104–up-regulated genes are pathogenesis related or may be involved in further signal amplification of defense signaling, such as *MKK4*, *RBOHD*, *ERF4*, *WRKY33*, *TGA1.3* (Table 1). Functional grouping revealed a high percentage (20%) of stress-responsive genes in the up-regulated genes, which represent only ≈8% in the repressed genes set, as is normally seen at the global genome level. Reciprocally, genes involved in signal transduction (& transcription regulation), normally of 4–5%, cover ≈20% among repressed genes (Fig. S4*B*). Thus, ERF104 targets several stress-related genes either directly and indirectly to coordinate stress responses.

Table 1. Selected genes upregulated in ERF104^{OE} plants

AGI code	Fold change*	*P* value†	TAIR description
Pathogenesis-related genes			
AT2G26020	1092	0.029	PDF1.2b
AT5G44420	869	0.020	PDF1.2
AT1G75040	10.7	0.036	PR5
AT5G36910	8.3	0.046	Thionin 2.2
AT1G19670	7.7	0.028	Coronatine-induced protein 1
AT3G05730	6.1	0.034	Defensin like
AT2G43590	3.2	0.049	Chitinase, put.
AT4G36010	3.1	0.038	Thaumatin family prot.
AT2G44490	3.1	0.034	PEN2
Defense signaling			
AT1G18570	35.9	0.013	MYB51
AT1G72920	10.1	0.045	Disease res. prot (TIR-NBS class)
AT3G04210	8.4	0.029	Disease res. prot (TIR-NBS class)
AT2G31230	7.6	0.049	ERF15
AT1G22070	5.8	0.046	TGA3
AT1G51660	4.8	0.036	MKK4
AT3G15210	4.6	0.046	ERF4
AT5G67280	4.2	0.025	RLK
AT2G38470	4.1	0.042	WRKY33
AT5G47910	3.7	0.039	RBOHD
AT5G52510	3.1	0.045	SCL8 scarecrow-like TF
AT1G32640	3	0.033	AtMYC2

*Fold changes are the ERF104^{OE}/Col-0 ratio.
†*P* values are corrected with 5% false discovery rate (FDR) multiple testing.

Responses Affected in Plants with Altered *ERF104* Expression. No difference in the ET-induced triple response was seen in the ERF104^{OE} plants (not shown). Although stronger symptoms developed, there was no enhanced bacterial growth after virulent *Pseudomonas syringae* infection (Fig. S5*A*). ERF overexpression often increases resistance to necrotrophic fungi (29–31). However, both disease symptom development and biomass quantification of *Botrytis cinerea* in the ERF104^{OE} plants showed a tendency toward greater susceptibility. Surprisingly, the *erf104* mutant showed the same trend (Fig. 5*B*).

To assess basal resistance, the non-adapted bacterial pathogen, *P. syringae* pv. phaseolicola (*Psp*) 1448A, which normally infects beans but not *Arabidopsis*, was tested. The *erf104* mutant and an RNAi line showed enhanced symptom development and more bacterial growth (Fig. 5*C*). The ERF104^{OE} plants also had higher *Psp* growth and a soaked lesion phenotype that resembles that seen during compatible interactions. Similarly, root growth inhibition by flg22 is enhanced in both the *erf104* mutant and ERF104^{OE}/ERF104m^{OE} plants (Fig. 5*D*). These results suggest that (*i*) the PAMP response that mediates resistance to non-adapted bacteria may be coordinated through flg22-mediated MPK6 activation and downstream components such as ERF104, and (*ii*) ERF104 is likely a vital component, as altering ERF104 expression in either direction changes the response.

Discussion

Mis-expression of key signal components often has severe phenotypic effects, and thus they are typically under tight control. Accordingly, ERF104 levels are regulated by mRNA stability (32) and phosphorylation-regulated protein stability (Figs. 4*A* and 6). ERF104 is exclusively phosphorylated by MPK6 but not MPK3 or MPK4 (Fig. 3) and, in analogy to the unique yeast MAPK substrates in mating/starvation pathways (33), may confer signal specificity. Thus, despite apparent functional redundancies, MPK3 and MPK6 must have separate non-redundant signaling roles.

Overexpression of ERF104 did not enhance disease resistance. In fact, both *erf104* and ERF104^{OE} showed reduced immunity against *B. cinerea* and the non-adapted *Psp* and enhanced the growth inhibition response to flg22 (Fig. 5 *B–D*). These results are difficult to explain but can only mean that ERF104 must be maintained at an optimal level and any alterations of this crucial threshold can tip the "signaling balance." For instance, it is possible that the ERF104^{OE} may sequestrate some ERF104-interactors into the nucleus (*cf.* MPK6, Fig. 1). In support of this, the root growth inhibition by flg22 (Fig. 5*D*) and the *Psp* response of the ERF104^{OE} (Fig. S5*B*) are reversed in the *mpk6* background, and thus dependent on MPK6. Taken together, the data are in agreement with a

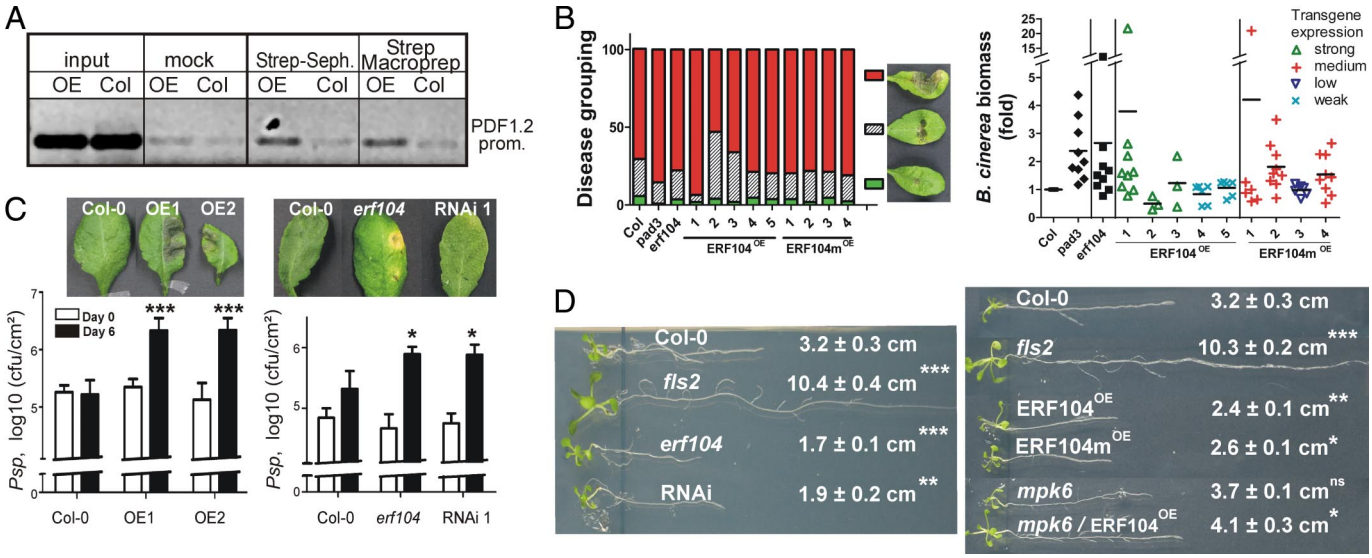

Fig. 5. Effects of modulating *ERF104* expression. (*A*) Chromatin immunoprecipitation (ChIP) shows higher levels of the *PDF1.2* promoter in immunoprecipitates of Strep-tagged ERF104 from ERF104^{OE} compared with Col-0 plants. (*B*) *Botrytis cinerea* disease progression, as monitored by symptom development in leaves (*left*) or biomass determination (*right*). Each biomass data point is an independent experiment, depicts fungal biomass in 18 leaf disks (with technical duplicates) and is shown as fold changes relative to Col-0 (horizontal dash indicates mean). The fungal biomass in the hypersusceptible mutant, *pad3*, is ≈2.3 fold higher. Note that enhanced susceptibility of the overexpressors seems to correlate with the transgene expression level (except for ERF104^{OE} line 2). (*C*) Both *erf104* and ERF104^{OE} show enhanced susceptibility to the bean pathogen, *P. syringae* pv. *phaseolicola* (infiltrated at 2×10^8 cfu/ml). *t* test *P* values: *<0.05, **<0.01, ***<0.001. (*D*) Root growth inhibition by flg22 (10 μM) is enhanced in plants with altered *ERF104* expression. Statistically significant differences (marked as in (*C*) in root length, compared with Col-0 roots, are indicated.

signal cascade involving flg22-mediated activation of MPK6 and downstream targets such as ERF104 to control defense responses.

An important finding in this report is the rapid disruption of ERF104/MPK6 complex, which implied that the flg22-triggered ET biosynthesis is faster (i.e., minutes, not hours) than previously reported (14). The discrepancy may lie in lower sensitivities of the "headspace capture" ET measurement method or in the differential accessibility of flg22 to protoplasts and leaf tissue. The speed of ET production may hint at it being upstream, where MPK6 is activated by ACC (12), but our data are compatible with it being downstream of MPK6 (see model, Fig. 6). Recently, ACC (200 μM for 1 hour) was shown to activate MPK6 in detached leaves, and a model is proposed wherein bifurcate pathways downstream of CTR1 antagonistically control EIN3 stability via two different phosphorylation sites (10) (Fig. 6). One of these pathways is thought to contain an MKK9 complex with MPK3/6. It should be noted that direct proof of a complex was not shown but deduced from the ability of MKK9 to activate MPK3/6 and that MPK3/6 activities are higher in a *ctr1* background, which can be suppressed by reintroducing active CTR1 (albeit a truncated CTR1). Another recent work showed that constitutively active MKK9 led to enhanced ET levels (25), which may explain some of the findings in (10). The conflicting data of the two groups on whether downstream responses are reduced by blocking ET signaling (e.g., by Ag^+ and AVG treatment) would need to be clarified (24). Nevertheless, this proposed CTR1/MKK9/MPKs pathway cannot account for the quick reaction we observe and accordingly, the ERF104/MPK6 complex disruption still occurred in *mkk9*-derived protoplasts (not shown).

Our current model is that the flg22 signal network includes one pathway for MPK6 to target ERF104 directly through phosphorylation and on a separate branch, to stimulate ET production, which triggers a yet unknown mechanism (that is dependent on EIN2 and the EIN3/EIL members) for the release of MPK6 from ERF104 in the nucleus (Fig. 6). It is conceivable that the continued binding of MPK6 to ERF104 might constrain physical interactions with subsequent ERF104 targets and impinge on its role in transcription activation. Along this line, Qiu et al. showed that flg22 and pathogen treatment caused the release of the MKS1/WRKY33 complex from MPK4; thus allowing WRKY33 to evoke camalexin

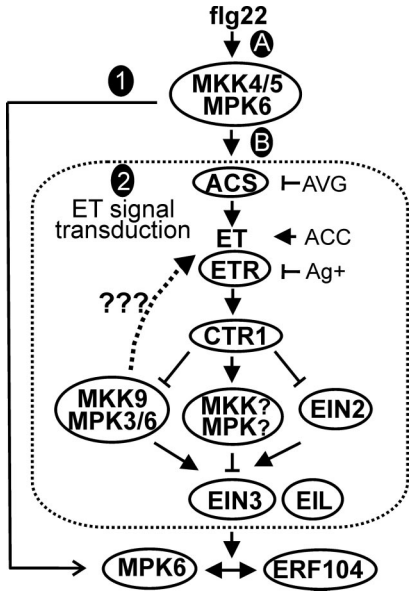

Fig. 6. Model of flg22 effect on MPK6/ERF104 interaction. The ERF104/MPK6 complex disruption requires flg22 stimulation of MPK6 activity (1) that also positively affects ERF104 stability, as well as ET signaling (2). The rapid ET signal may be upstream (*A*) or downstream (*B*) of MPK6 activation; but the inhibitor/mutant analyses support the latter. Yoo et al. reported bifurcate pathways downstream of ETR (ET receptors) and CTR1, one of which includes MKK9, to antagonistically control EIN3 stability (10). Question marks denote the report that active MKK9 can raise ET levels to feedback positively into ET signaling (25); but this conflicts with results reported by Yoo et al. (10). The ERF104/MPK6 complex disruption by flg22 is independent of the MKK9 pathway but dependent on EIN2 and EIN3/EIL (EIN3-like) proteins.

production by targeting the *PAD3* promoter (20). However, unlike our data, the release of MKS1/WRKY33 is independent of substrate (MKS1) phosphorylation and the timing of the complex disruption was not provided, so that it is not clear whether it is as rapid as reported here. Moreover, additional factors are probably involved, because flg22 alone does not induce camalexin production and "altered *PAD3* expression in *mks1* is insufficient to affect camalexin production" (20). *WRKY33* expression is enhanced in ERF104^{OE} (Table 1), so that components downstream of MPK6 signaling may feed into the MPK4 pathway, thus linking the two opposing branches of flg22-regulated MAPK pathways that control defense responses.

In summary, transcription factor release may be a common theme after MAPK activation to control downstream gene expression. We further showed that ET signaling is required to mediate such substrate release, and it is tempting to speculate that other phytohormones may similarly control protein–protein interactions to coordinate downstream responses.

Materials and Methods

Additional methods are given in the *SI Text*.

FRET Analysis. Protoplast isolation and transfection were performed as described in (3, 19). FRET measurements were done with YFP/CFP fusion proteins, using a LSM 510 Meta confocal microscope (Zeiss) in the channel mode (setup: CFP filter, 473.3–505.4 nm; YFP emission filter, 516.1–548.2 nm). The acceptor photobleaching method (21) was used. For every analysis, 12 or more protoplasts (i.e., the minimal number for performing Kolmogorov-Smirnov test; see below) were analyzed and scanned at 458 nm twice before and twice after bleaching of the YFP (full laser power, 514 nm, 80 times). The relative fluorescence intensity (I) in a certain region of interest (ROI) was measured using the ROI mean function of the Zeiss software. FRET efficiency (E_F) was then calculated with the following equation:

$$E_F = (I_{\text{after bleaching}} - I_{\text{before bleaching}}) \times 100/I_{\text{after bleaching}}$$

The following statistical analysis was performed to evaluate the considerable variation in E_F within each data series. First, Gaussian distribution of the data points was established using the Kolmogorov-Smirnov test, followed by removal of outliers via Grubb's test (GraphPad Prism software package), followed by a Mann-Whitney significance analysis ($P < 0.05$) against both positive and negative controls.

Protein Work. Protein extraction, immunoprecipitation (α-MAPK or α-GFP [BD Living Colors]), *in vitro* phosphorylation reactions with the indicated substrates were performed as described (18). ERF104 stability was tested after incubating leaves with 100 μM cycloheximide (±10 μM flg22), and visualized with α-Strep-Tactin HRP conjugate (IBA-BioTAGnology, Germany) in Western blots.

Microarray Hybridization and Analysis. Six-week old Col-0, *erf104*, *mpk6* and ERF104^{OE} plants were infiltrated with 1 μM flg22 or H_20 and harvested 4 hours later. Total RNA was processed according to the Affymetrix protocol for biotin-labeled cRNA and hybridized to the Affymetrix ATH1 chip. The data were analyzed with Genespring GX 7.3.1 software (Agilent) with the following parameters: Filter on Flags for present or marginal in 50% of all considered experiments, Filter for reliable differentially expressed genes based on volcano plot ($P < 0.05$ and >3-fold change in expression). Moreover, a Benjamini-Hochberg false discovery rate (FDR) of 5% was implemented. For the flg22 experiments, analysis for each genotype was separately performed and a composite list of flg22-regulated genes compiled, with the aim of including genes that may be differentially regulated in the genotype. Global expression profile was visualized by k-means clustering and condition tree (Genespring). Microarray data for JA and ET were obtained from public databases (GARNET, Genevestigator).

ACKNOWLEDGMENTS. We thank Simone Altmann, Joseph Ecker, Bettina Hause, Kai Naumann, Thorsten Nürnberger, Ralph Panstruga, Stefan Posch, Sabine Rosahl, Ralf Reski, Jen Sheen, Imre Somssich, and Bernhard Westermann for sharing advice, materials, and protocols. This work was financed by the German Research Foundation within the SFB648 program.

1. Gustin MC, Albertyn J, Alexander M, Davenport K (1998) MAP kinase pathways in the yeast *Saccharomyces cerevisiae*. *Microbiol Mol Biol Rev* 62:1264–1300.
2. Nakagami H, Pitzschke A, Hirt H. (2005) Emerging MAP kinase pathways in plant stress signalling. *Trends Plants Sci* 10:339–346.
3. Asai T, et al. MAP kinase signalling cascade in *Arabidopsis* innate immunity (2002) *Nature* 415:977–983.
4. Ichimura K, et al. (2006) MEKK1 is required for MPK4 activation and regulates tissue-specific and temperature-dependent cell death in Arabidopsis. *J Biol Chem* 281:36969–36976.
5. Suarez-Rodriguez MC, et al. (2007) MEKK1 is required for flg22-induced MPK4 activation in Arabidopsis plants. *Plant Physiol* 143:661–669.
6. Kroj T, et al. (2003) Mitogen-activated protein kinases play an essential role in oxidative burst-independent expression of pathogenesis-related genes in parsley. *J Biol Chem* 278:2256–2264.
7. Petersen M, et al. (2000) *Arabidopsis* MAP kinase 4 negatively regulates systemic acquired resistance. *Cell* 103:1111–1120.
8. Bari R, Jones JD (2008) Role of plant hormones in plant defence responses. *Plant Mol Biol* 69:473–488.
9. Zhang S, Klessig DF. Salicylic acid activates a 48-kD MAP kinase in tobacco (1997) *Plant Cell* 9:809–824.
10. Yoo SD, et al. (2008) Dual control of nuclear EIN3 by bifurcate MAPK cascades in C2H4 signalling. *Nature* 451:789–795.
11. Takahashi F, et al. (2007) The mitogen-activated protein kinase cascade MKK3-MPK6 is an important part of the jasmonate signal transduction pathway in *Arabidopsis*. *Plant Cell* 19:805–818.
12. Ouaked F, Rozhon W, Lecourieux D, Hirt H. (2003) A MAPK pathway mediates ethylene signaling in plants. *EMBO J* 22:1282–1288.
13. Kumar D, Klessig DF (2000) Differential induction of tobacco MAP kinases by the defense signals nitric oxide, salicylic acid, ethylene, and jasmonic acid. *Mol Plant Microbe Interact* 13:347–351.
14. Liu Y, Zhang S (2004) Phosphorylation of 1-aminocyclopropane-1-carboxylic acid synthase by MPK6, a stress-responsive mitogen-activated protein kinase, induces ethylene biosynthesis in Arabidopsis. *Plant Cell* 16:3386–3399.
15. Joo S, Liu Y, Lueth A, Zhang S (2008) MAPK phosphorylation-induced stabilization of ACS6 protein is mediated by the non-catalytic C-terminal domain, which also contains the cis-determinant for rapid degradation by the 26S proteasome pathway. *Plant J* 54:129–140.
16. Menke FL, et al. (2005) Tobacco transcription factor WRKY1 is phosphorylated by the MAP kinase SIPK and mediates HR-like cell death in tobacco. *Mol Plant Microbe Interact* 18:1027–1034.
17. Andreasson E, et al. (2005) The MAP kinase substrate MKS1 is a regulator of plant defense responses. *EMBO J* 24:2579–2589.
18. Ahlfors R, et al. (2004) Stress hormone-independent activation and nuclear translocation of mitogen-activated protein kinases in *Arabidopsis thaliana* during ozone exposure. *Plant J* 40:512–522.
19. Lee J, Rudd JJ, Macioszek VK, Scheel D (2004) Dynamic changes in the localization of MAPK cascade components controlling pathogenesis-related (PR) gene expression during innate immunity in parsley. *J Biol Chem* 279:22440–22448.
20. Qiu JL, et al. (2008) Arabidopsis MAP kinase 4 regulates gene expression through transcription factor release in the nucleus. *EMBO J* 27:2214–2221.
21. Karpova TS, et al. (2003) Fluorescence resonance energy transfer from cyan to yellow fluorescent protein detected by acceptor photobleaching using confocal microscopy and a single laser. *J Microsc* 209:56–70.
22. Meindl T, Boller T, Felix G (2000) The bacterial elicitor flagellin activates its receptor in tomato cells according to the address-message concept. *Plant Cell* 12:1783–1794.
23. Felix G, Duran JD, Volko S, Boller T (1999) Plants have a sensitive perception system for the most conserved domain of bacterial flagellin. *Plant J* 18:265–276.
24. Hahn A, Harter K (2008) MAP kinase cascades and ethylene—signaling, biosynthesis or both? *Plant Physiol* 149:1207–1210.
25. Xu J, et al. (2008) Activation of MAPK kinase 9 induces ethylene and camalexin biosynthesis and enhances sensitivity to salt stress in Arabidopsis. *J Biol Chem* 283:26996–27006.
26. Nakano T, Suzuki K, Fujimura T, Shinshi H (2006) Genome-wide analysis of the ERF gene family in *Arabidopsis* and rice. *Plant Physiol* 140:411–432.
27. Kinoshita E, Kinoshita-Kikuta E, Takiyama K, Koike T (2006) Phosphate-binding tag, a new tool to visualize phosphorylated proteins. *Mol Cell Proteomics* 5:749–757.
28. Rushton PJ, et al. (2002) Synthetic plant promoters containing defined regulatory elements provide novel insights into pathogen- and wound-induced signaling. *Plant Cell* 14:749–762.
29. Lorenzo O, Piqueras R, Sanchez-Serrano JJ, Solano R (2003) Ethylene response factor1 integrates signals from ethylene and jasmonate pathways in plant defense. *Plant Cell* 15:165–178.
30. Pre M, et al. (2008) The AP2/ERF domain transcription factor ORA59 integrates jasmonic acid and ethylene signals in plant defense. *Plant Physiol* 147:1347–1357.
31. McGrath KC, et al. (2005) Repressor- and activator-type ethylene response factors functioning in jasmonate signaling and disease resistance identified via a genome-wide screen of *Arabidopsis* transcription factor gene expression. *Plant Physiol* 139:949–959.
32. Gutierrez RA, Ewing RM, Cherry JM, Green PJ (2002) Identification of unstable transcripts in *Arabidopsis* by cDNA microarray analysis: Rapid decay is associated with a group of touch- and specific clock-controlled genes. *Proc Natl Acad Sci USA* 99:11513–11518.
33. Bao MZ, et al. (2004) Pheromone-dependent destruction of the Tec1 transcription factor is required for MAP kinase signaling specificity in yeast. *Cell* 119:991–1000.